Original Article

Hounsfield Units: A new indicator showing maxillary resistance in rapid maxillary expansion cases?

Yasemin Bahar Acar[a]; Melih Motro[b]; A. Nejat Erverdi[c]

ABSTRACT

Objective: To determine if density measurements of several maxillary regions in Hounsfield Units (HU) and outcomes of rapid maxillary expansion (RME) are correlated. Is correlation powerful enough to give us direct information about maxillary resistance to RME?

Materials and Methods: Twenty-two computed tomographic (CT) scans (14 years) are used in this archive study. Two CT records were collected, one before RME (T_1) and one after 3 months of retention period (T_2). Maxillary measurements were made using dental and skeletal landmarks in first molar and first premolar slides to measure the effects of RME. Density of midpalatal suture (MPSD) and segments of maxillary bone is measured in HU at T_1. Correlation analysis was conducted between density measurements and maxillary variables. Regression analysis was then performed for variables that showed positive correlation.

Results: There was no correlation between density and skeletal measurements. Intermolar angle (ImA) in molar slice showed statistically significant correlation with density measurements. The ImA variable showed the highest correlation with MPSD in frontal section ($r = 0.669$, $P < .01$).

Conclusions: There is correlation of 32.1–43.3% between density measurements and ImA increase. Our density measurements explain a certain percentage of ImA increase, but density is not the only and definitive indicator of changes after RME. (*Angle Orthod.* 2015;85:109–116.)

KEY WORDS: Rapid maxillary expansion; Hounsfield Units; Suture density

INTRODUCTION

Rapid maxillary expansion (RME) is a widely used orthopedic procedure designed to increase maxillary transverse dimension in young patients by midpalatal and circumferential sutural opening. Maxillary expansion is recommended in certain clinical situations unless there is a systemic contraindication. By contrast, the decision to use surgically assisted RME (SARME) is not as easy, especially in young adults. With increasing age, the resistance of the maxilla to expansion increases as a result of three major causes: midpalatal synostosis, midpalatal interlocking, and circummaxillary rigidity.[1] These important factors are clinically unmeasurable.

There are several proposed techniques to assist clinicians in choosing surgical assistance, including skeletal maturity assessment by hand-wrist radiography or cervical vertebra maturation[2,3] and midpalatal suture assessment before and after RME by occlusal radiography.[4] However, neither of these methods serves as a definitive indicator for SARME, and more importantly, these methods do not provide a direct evaluation of the maxillofacial area.

In orthodontics, three-dimensional (3D) imaging is indicated for numerous situations, such as the evaluation of impacted teeth,[5] bone graft evaluation in cleft regions,[6] alveolar bone analysis prior to placing temporary orthodontic anchorage devices,[7] and assessment of the impact of RME on nasomaxillary structures.[8] Computed tomography (CT) allows mineral density quantification in specific jaw sites in Hounsfield Units (HU) based on grayscale differences. This property of CT has been widely used, especially in the field of implantology, and is applicable to orthodontics.

[a] Resident, Department of Orthodontics, School of Dentistry, University of Marmara, Istanbul, Turkey.

[b] Research Assistant, Department of Orthodontics, School of Dentistry, University of Marmara, Istanbul, Turkey.

[c] Professor, Department of Orthodontics, School of Dentistry, University of Marmara, Istanbul, Turkey.

Corresponding author: Dr Yasemin Bahar Acar, Faculty of Dentistry, Department of Orthodontics, Marmara University, Büyükçiftlik Sokak. No: 6 Nişantaşı, Şişli, İstanbul, Turkey (e-mail: yaseminbaharciftci@gmail.com)

Accepted: March 2014. Submitted: November 2013.
Published Online: May 1, 2014

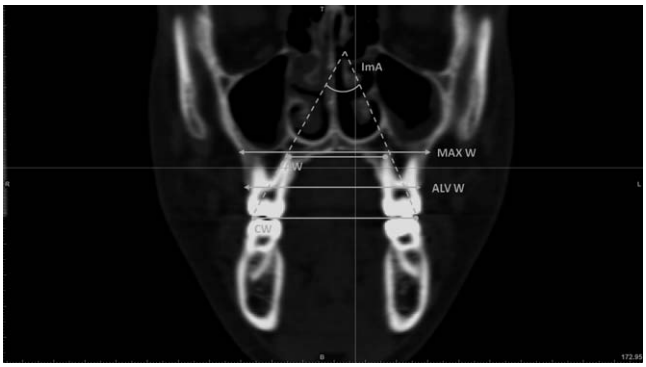

Figure 1. Dental and skeletal measurements.

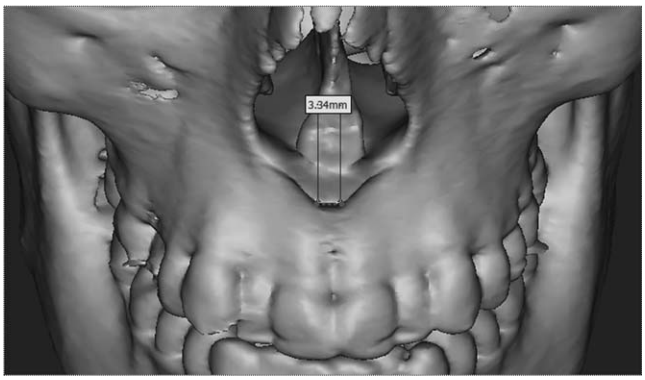

Figure 2. Measuring ANS width postexpansion.

The present study assesses the relationship between the CT density of several maxillary regions and the RME outcomes and determines the diagnostic utility of CT density in predicting maxillary resistance to RME. CT may potentially prove beneficial for clinicians choosing corticotomy, and it may provide measurable diagnostic information related to the maxillofacial area. SARME is a time- and energy-intensive procedure for the clinician and an invasive and costly procedure for the patient; therefore, the ability to thoroughly assess the need for SARME will benefit both.

MATERIALS AND METHODS

The parents of each patient provided informed consent to participate in the study, which was approved by the ethical committee of Marmara University, Institute of Health Sciences. Archived CT scans of 22 patients (11 males, 11 females; mean age: 14.25 years) at the Marmara University Dental Faculty, Department of Orthodontics, were evaluated retrospectively. The inclusion criteria were as follows: patients must be aged 11–17 years and have maxillary constriction with bilateral posterior crossbite, permanent dentition, no systemic disease, no previous orthodontic treatment, and no periodontal disease history.

RME was performed in each patient as a part of the orthodontic treatment comprising an acrylic–cap splint-type hyrax appliance, rigid bonded expansion appliance with a hyrax screw in the palate, and an acrylic cap splint covering the palatal and occlusal premolar and molar surfaces. The appliance was bonded using dual-cure glass-ionomer cement. Patients were instructed to activate the screw twice daily. Expansion was continued until the upper first molar palatal cusp tips touched the lower first molar buccal cusps; the amount of expansion was monitored at weekly examinations. At the end of the active expansion phase, the hyrax screw was stabilized with a stainless-steel ligature wire and flowable composite. The appliance remained in the mouth for 3 months to ensure retention. Afterwards, the expansion appliance was removed, and a transpalatal arch (TPA) with arms extending from the molar bands to the premolars was immediately cemented to further ensure retention.

Two CT records were collected from each patient, one before RME (T_1) and one after the 3-month retention period (T_2). The second CT was performed after removing the acrylic cap splint and before placing the TPA to prevent metallic artifacts that can influence imaging quality and diagnostic accuracy. CTs were collected at the same hospital using a spiral CT machine (Siemens Sensation 40, Siemens Medical Solutions of Siemens, Erlangen, Germany) at 120 kV, 80 mAs, with a 12.6 $\times$ 12.6-cm field of view and a 512 $\times$ 512-pixel matrix. Axial 0.3-mm increment slices comprising the entire cranium were obtained. Dicom CT data were analyzed with 3D prototyping software (Mimics v.16.0, Materialise, Leuven, Belgium). A specialized pillow and two perpendicular laser light beams stabilized and standardized the head position during scanning. The horizontal beam was adjusted parallel to the Frankfurt horizontal plane, and the vertical beam passed through the midsagittal plane.

The RME maxillary effects were measured using dental and skeletal landmarks (Figures 1 and 2) and compared between pre- and postexpansion coronal images. Dental and skeletal measurements were obtained from the coronal images passing through the center of the maxillary first molar and premolar palatal root apices. Bone density was measured only on pre-expansion CTs.

Dental Measurements

The following parameters were measured: apical width (AW)—the distance between the maxillary first molar palatal root apices; crown width (CW)—the distance between the maxillary first molar mesiobuccal cusp tips; and intermolar angle (ImA)—the angle between the maxillary first molar axes (molar axis

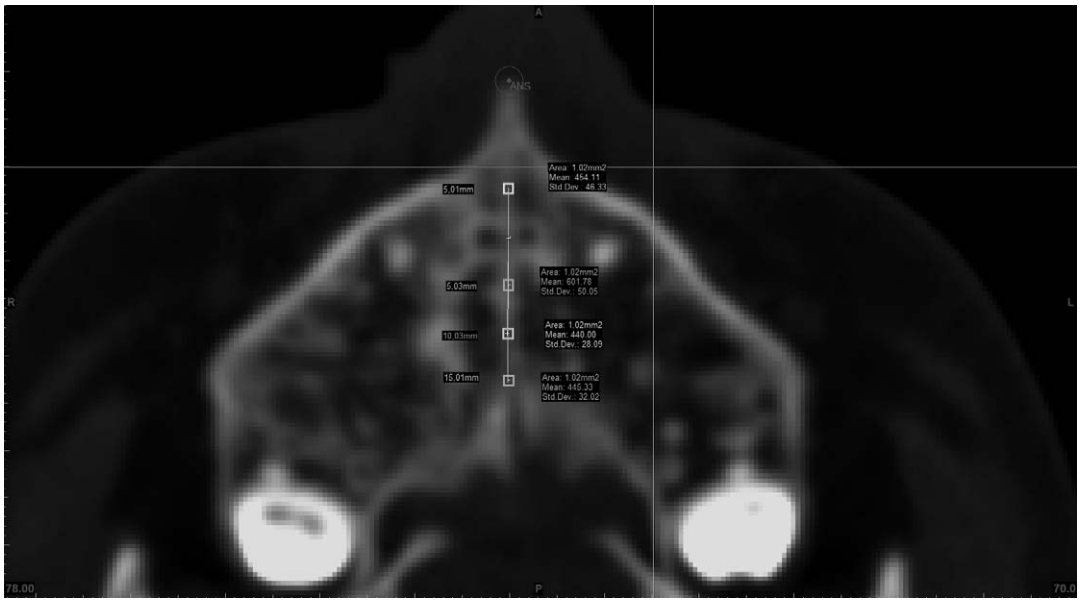

Figure 3. MPSD axial measurements at points A, P1, P2, and P3.

defined as the line connecting the palatal root apex and mesiobuccal cusp tip of the maxillary first molar) (Figure 1).

Skeletal Measurements

The following skeletal parameters were measured: anterior nasal spine width (ANSW)—the distance between the right and left anterior nasal spine points measured on 3D skull images (Figure 2); alveolar width (AlvW)—the width between the most coronal points of the maxillary first molar buccal alveolar crest; and maxillary width (MaxW)—the width between the maxillary buccal cortexes of the maxillary first molars, tangent to the hard palate.

Density Measurements

Midpalatal suture density on axial cut. On axial slice passing through the ANS and midpalatal suture, the center of the incisive foramen was marked as ''O.'' Points at 5 mm anterior (point A) and 5, 10, and 15 mm posterior (P1, P2, and P3, respectively) to ''O'' were also marked. Then, 1-mm^2 squares were drawn at A, P1, P2, and P3. The square area densities were

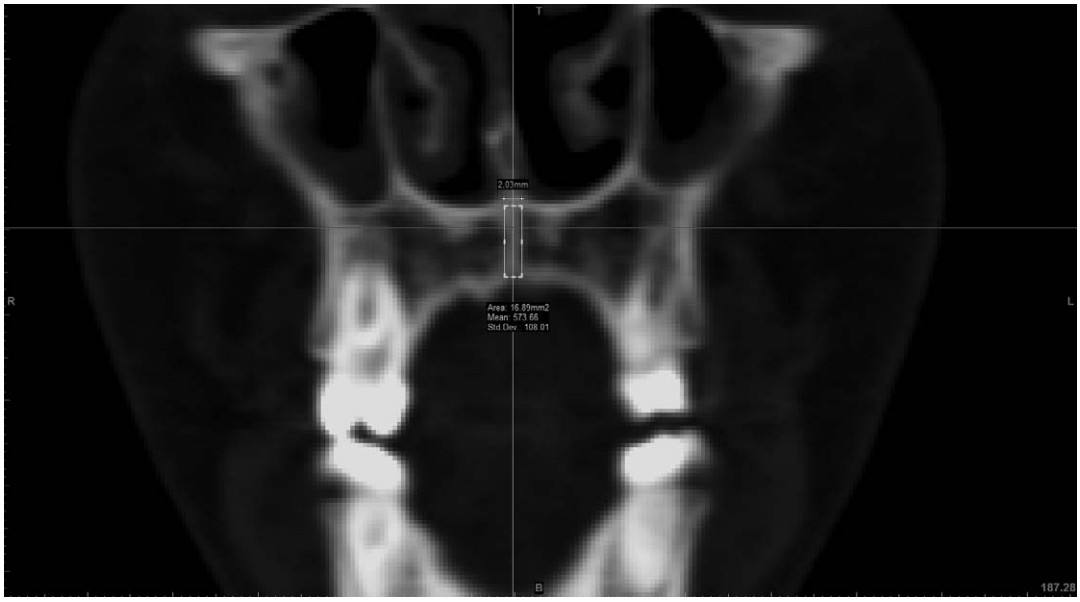

Figure 4. MPSD frontal measurement at P2.

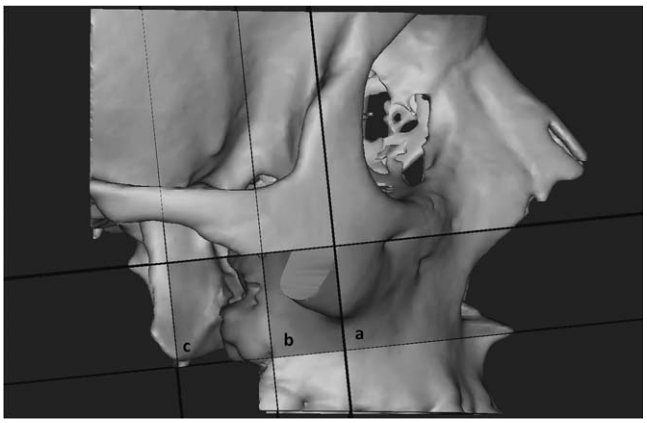

Figure 5. Maxillary buttress 3D model shown with cutting planes (a: anterior; b: middle; c: posterior).

measured, averaged, and recorded as the midpalatal suture density on axial cut (MPSD axial) (Figure 3).

MPSD frontal. A 2-mm-wide rectangle was drawn on the midpalatal suture on the frontal view, limited by the nasal floor cortex superiorly and the palatal vault cortex inferiorly and centered on the midsagittal reference line. The rectangle density was measured at points A, P1, P2, and P3, and the average was recorded as the MPSD on frontal cut (MPSD frontal) (Figure 4).

Maxillary buttress. 3D skull images were obtained in the following planes: lateral, two planes (right and left) parallel to the midsagittal plane and passing through the most superior point to the frontomaxillary sutures; inferior, the plane passing through the ANS and the most proximal points of the right and left pterygoid hamulus (designated as the ANS-Sphenoid plane); posterior, the plane perpendicular to the ANS-Sphenoid plane and passing through the most proximal points of the right and left medial sphenoid bone plates; and superior, the plane parallel to the ANS-Sphenoid plane and passing through the right infraorbital foramen.

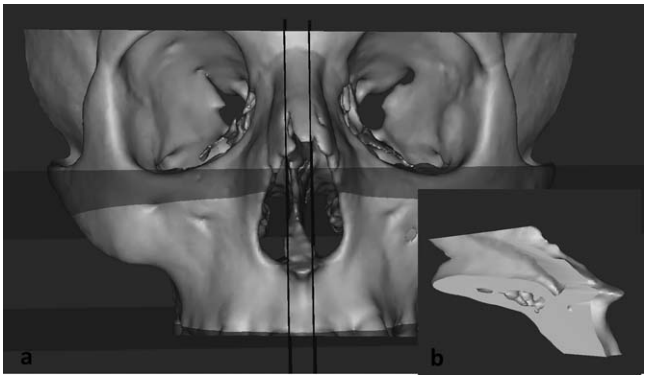

Figure 6. (a) Midpalatal suture 3D model shown before removal of vomer. (b) Oblique view.

Table 1. Density measurements in Hounsfield Units (HU)[a]

Density Measurements, HU	Minimum	Maximum	Average	±SD
MPSD axial	485.3	885.56	702.9	113.5
MPSD frontal	462.48	863.25	648.62	106.43
Max buttress				
Anterior	496.3	937.7	694.23	121.63
Middle	470.3	963.2	669.46	138.53
Posterior	491.99	883.9	654.15	117.34
MIDPAL 3D	488.3	855.2	683.37	99.73

[a] SD indicates standard deviation; MPSD, density of midpalatal suture; Max buttress, maxillary buttress; and MIDPAL 3D, midpalatal suture in three dimensions.

The resultant bone model was divided into three parts, anterior, middle, and posterior, by two vertical planes passing through the greater palatinal foramen and zygomatic process (Figure 5). Dental structures remaining in the models were erased from the image, and the bone density was recorded.

Midpalatal suture in 3D. The 3D skull reconstruction was divided by two planes parallel to the midsagittal plane and passing 3 mm lateral to the ANS bilaterally (Figure 6). Vomer and dental structures were erased, and the bone density was recorded.

Statistical Analyses

The SPSS for Windows 15.0 (SPSS, Chicago, Ill) program was used for statistical analyses. Descriptive statistical methods (mean, standard deviation [SD]) and pre-/postexpansion quantitative data were compared using the paired samples *t*-test. Normally distributed data were analyzed with the Pearson correlation analysis; data not normally distributed were analyzed with the Spearman's rho correlation analysis. A simple regression analysis assessed the relationship between bone density and the ImA increase. Data reliability was assessed by the intraclass correlation coefficient (ICC). Results were evaluated at a $P < .05$ significance level and a 95% confidence interval.

RESULTS

The bone density minimum, maximum, mean, and SD are summarized in Table 1. Table 2 summarizes the mean, SD, and significance values of pre- and postexpansion dental and skeletal measurements. There were significant differences in the pre- and postexpansion values of all of the variables evaluated ($P < .01$). Density, skeletal, and dental measurements were also evaluated according to gender and age (mean age: 14 years; group 1, <14 years; group 2, >14 years). There were no statistically significant differences ($P > .05$) between male and female

Table 2. Mean and Standard Deviation (SD) Values of Skeletal and Dental Variables[a]

	Pre-expansion		Postexpansion		Change		
Variables	Mean	SD	Mean	SD	Mean	SD	*P*
ANSW	1.02	0.98	3.07	0.85	2.04	1.11	.001**
Maxillary first molar slice							
AW	31.35	2.82	35.44	2.22	4.08	2.24	.001**
CW	47.31	3.72	54.6	3.21	7.28	2.17	.001**
ImA	43.57	9.91	53.29	9.09	9.72	7.62	.001**
MaxW	61.02	3.1	63.04	3.05	2.01	1.18	.001**
AlvW	52.7	3.04	58.36	2.74	5.66	1.84	.001**
Maxillary first premolar slice							
AW	31.1	2.08	35.8	2.29	4.7	1.95	.001**
CW	37.03	3.88	44.49	3.5	7.46	2.21	.001**
ImA	18.06	7.72	26.08	9.92	8.02	7.15	.001**
MaxW	41.43	3.39	44.21	3.16	2.78	2.03	.001**
AlvW	41.49	2.82	47.39	2.35	5.89	2.27	.001**

[a] ANSW indicates anterior nasal spine width; AW, apical width; CW, crown width; ImA, intermolar angle; MaxW, maxillary width; and AlvW, alveolar width.

** indicates $P < 0.01$.

subjects or between subjects <14 and >14 years of age.

The correlation analyses for all of the variables are shown in Tables 3 and 4. The ImA molar slice showed a statistically significant correlation with all density measurements and was the most correlated with the MPSD frontal. There was a significant ($P < .01$) 66.9% correlation between the ImA increase and the MPSD frontal value. To ascertain the power of each density measurement on the ImA increase a regression analysis was performed for the ImA (molar) and density measurements. Correlation between bone density and other variables was not consistent, and therefore a regression analysis was not performed.

The regression analysis between the MPSD axial and ImA (Table 5) yielded an R^2 value of 0.321, indicating that 32.1% of the ImA change can be attributed to the MPSD axial value (Table 5A). This model is statistically significant ($P = .006$; $P < .01$) (Table 5B). Table 5C shows the estimated coefficients and *t* values. A 1-unit increase in the MPSD axial value caused a 0.036× ImA increase. The *t* value for this coefficient was statistically significant. The final model is represented by the following equation:

$$\text{ImA increase} = -14.844 + 0.036 \times (\text{MPSD axial}).$$

The R^2 values corresponding to each density measurement and resulting equation model are summarized in Table 6. The MPSD 3D had the greatest effect on the ImA, with an $R^2 = 43.3\%$.

All measurements were repeated by the same observer 3 months later. The ICC was close to 1.00. The method error evaluation is shown in Table 7. Density measurements and maxillary measurements were reliable and reproducible with an insignificant error and without affecting the results.

Table 3. Correlation Analysis Between Density and Maxillary Variables in Molar Slice[a]

	Molar Slice											
	ANSW		MaxW		AlvW		AW		CW		ImA	
	r	*P*	*r*	*P*	*r*	*P*	*r*	*P*	*r*	*P*	*r*	*P*
MPSD axial	−0.169	.451	0.292	.187	0.383	.079	−0.174	.437	0.377	.084	**0.573**	**.005****
MPSD frontal	−0.265	.234	−0.041	.855	0.135	.549	**−0.425**	**.049***	0.286	.197	**0.669**	**.001****
Max buttress												
Anterior	**−0.497**	**.019***	**0.512**	**.015***	0.188	.403	−0.299	.177	0.257	.249	**0.568**	**.006****
Middle	**−0.460**	**.031***	**0.469**	**.028***	0.116	.606	−0.336	.126	0.218	.330	**0.584**	**.004****
Posterior	−0.387	.076	**0.567**	**.006****	0.285	.198	−0.143	.526	0.380	.081	**0.545**	**.009****
MIDPAL 3D	**−0.424**	**.049***	0.277	.212	0.145	.521	−0.296	.180	0.381	.080	**0.654**	**.001****

[a] ANSW indicates anterior nasal spine width; MaxW, maxillary width; AlvW, alveolar width; AW, apical width; CW, crown width; ImA, intermolar angle; MPSD, density of midpalatal suture; and MIDPAL 3D, midpalatal suture in three dimensions.

* indicates $P < 0.05$; ** indicates $P < 0.01$; Bold indicates statistically significant results.

Table 4. Correlation Analysis Between Density and Maxillary Variables in Premolar Slice[a]

	Premolar Slice									
	MaxW		AlvW		AW		CW		ImA	
	r	*P*	*r*	*P*	*r*	*P*	*r*	*P*	*r*	*P*
MPSD axial	0.030	.895	0.244	.273	0.031	.891	0.406	.061	**0.430**	**.046***
MPSD frontal	−0.265	.234	0.051	.820	−0.221	.323	0.331	.132	**0.585**	**.004****
Max buttress										
Anterior	−0.014	.952	0.282	.204	−0.024	.917	0.314	.154	0.218	.331
Middle	0.041	.855	0.254	.255	−0.058	.797	0.288	.193	0.241	.280
Posterior	0.033	.883	**0.425**	**.049***	0.146	.516	**0.426**	**.048***	0.229	.305
MIDPAL 3D	−0.237	.289	0.216	.334	−0.042	.852	**0.425**	**.048***	**0.476**	**.025***

[a] MaxW, maxillary width; AlvW, alveolar width; AW, apical width; CW, crown width; ImA, intermolar angle; MPSD, density of midpalatal suture; and MIDPAL 3D, midpalatal suture in three dimensions.

* $P < .05$; ** $P < .01$; Bold indicates statistically significant results.

DISCUSSION

In current orthodontic dentistry, there are protocols guiding clinicians to choose between RME and SARME. However, studies investigating suture maturation have offered conflicting interpretations of the clinical principles used to evaluate skeletal age radiographically. A study by Schlegel et al.[9] found that the youngest donor with ossification was 23 years old, yet a 50-year-old patient did not have ossification. Persson and Thilander[10] reported that palatal sutures may become obliterated during the juvenile period, but a marked closure was rare prior to the third decade of life. They found the earliest closure in a 15-year-old girl, and bony spicules appear to have been observed between the ages of 15 and 19 years. Notably, only 5% of sutures are closed by 25 years, and 5% of suture closures with mechanical interlocking and circummaxillary rigidity can be broken without a corticotomy.[1] In a more recent microcomputed tomography study, Korbmacher et al.[11] concluded that the suture obliteration index was generally low, varied between individuals, and did not correlate with chronological age. Interdigitation was also independent of age. Collectively, these histological results indicate that there is a wide range for the corticotomy upper age limit, which is especially

Table 5. Effect of Density of Midpalatal Suture (MPSD) Axial on Intermolar Angle (ImA) Increase

A. Model Summary

	Model Summary[a]			
Model	*R*	R^2	Adjusted R^2	Standard Error of the Estimate
1	.567[b]	.321	.287	6.44147

[a] Dependent variable: ImA increase.

[b] Predictors: (constant), MPSD axial.

B. Variance Analysis

		ANOVA[a]				
Model		Sum of Squares	df	Mean Square	*F*	Significance
1	Regression	392.587	1	392.587	9.462	.006[b]
	Residual	829.851	20	41.493		
	Total	1222.438	21			

[a] Predictors: (Constant), MPSD axial.

[b] Dependent variable: ImA increase.

C. Parameter Estimates

		Coefficients[a]				
		Unstandardized Coefficients		Standardized Coefficients		
Model		B	Standard Error	Beta	*t*	Significance
1	(Constant)	−14,844	8.104		−1.832	.082
	Midpalatal suture, axial	.036	.012	.567	3.076	.006

[a] Dependent variable: intermolar angle (ImA) increase.

Table 6. Summary of Regression Analyses[a]

HU	R^2	Model
MPSD axial	0.321	ImA = −14.844+0.036(x) (MPSD axial)
MPSD frontal	0.427	ImA = −20.647+0.047* (MPSD frontal)
Anterior max buttress	0.355	ImA = −16.211+0.037* (anterior)
Middle max buttress	0.409	ImA = −13.850+0.035* (middle)
Posterior max buttress	0.386	ImA = −16.712+0.040* (posterior)
MPSD 3D	0.433	ImA = −24.691+0.050* (MPSD 3D)

[a] HU indicates Hounsfield Units; max buttress, maxillary buttress; MPSD, density of midpalatal suture; 3D, three dimensional; and ImA, intermolar angle.

Table 7. Evaluation of the Method Error[a]

	ICC	95% CI	*P*
ANS			
Pre	0.828	0.482–0.951	.001**
Post	0.936	0.782–0.982	.001**
MaxW			
Pre	0.904	0.685–0.973	.001**
Post	0.877	0.609–0.965	.001**
AlvW			
Pre	0.965	0.875–0.990	.001**
Post	0.905	0.687–0.973	.001**
AW			
Pre	0.838	0.506–0.954	.001**
Post	0.866	0.580–0.962	.001**
CW			
Pre	0.974	0.906–0.993	.001**
Post	0.957	0.847–0.988	.001**
ImA			
Pre	0.996	0.986–0.999	.001**
Post	0.992	0.971–0.998	.001**
Midpalatal suture axial	0.875	0.603–0.965	.001**
Midpalatal suture frontal	0.986	0.949–0.996	.001**
Anterior max buttress	0.964	0.872–0.990	.001**
Middle max buttress	0.990	0.963–0.997	.001**
Posterior max buttress	0.987	0.952–0.996	.001**
Midpalatal suture 3D	0.979	0.923–0.994	.001**

[a] ICC indicates intraclass correlation coefficient; CI, confidence interval; ANS, anterior nasal spine; MaxW, maxillary width; AlvW, alveolar width; AW, apical width; CW, crown width; ImA, intermolar angle; and 3D, three dimensional.

** $P < .01$.

critical between the ages of 15 and 25 years. At present, the potential benefit from RME cannot be firmly predicted even in patients over 15 years of age prior to attempting the expansion clinically.

CT is widely used in implant dentistry because it offers a 3D analysis that enables mineral density quantification at specific jaw sites in HU.[12] Several comparative studies confirmed the reliability and high accuracy of 3D CT for quantitative and qualitative analyses[13–15] and concluded that CT is a valuable diagnostic supplement to subjective bone density evaluation.[16–18] Cone beam computed tomography (CBCT) is preferred in dentistry as a result of the lower radiation dose it affords compared to that required in standard CT. However, standardization between CBCT machines is low,[7] which causes Hounsfield scale variability. Therefore, despite the lower radiation dose, CBCT is unreliable for comparing and measuring the HU. Although CT is not in routine use either for orthodontics or research, its suitability for measuring density makes it the modality of choice in this study. Regardless, the decision to perform CT should be limited to cases in which low-dose CBCT is inadequate.

Head orientation was poor in some subjects, despite precautions to stabilize it. This can be overcome during distance and angular measurements by using well-defined anatomic references. However, poor cranium orientation particularly affected the suture density measurements on sectional views because the suture is a fine line and requires more precise measurement. Digital reorientation can be performed, but this maneuver decreases image quality and was thus avoided. Images were evaluated without reorientation, which may have introduced error in the sectional view density measurements of some subjects.

Expansion forces are transmitted to the midface and craniofacial complex through the zygomaticomaxillary, pterygomaxillary, and nasomaxillary resistance areas. A reactive force, called the buttressing effect, develops against the expansion forces according to patient age and the circummaxillary bone rigidity. Investigators vary in their opinions of this issue. Haas[19] reports that pressure is generated by the alveolar processes, palatal vault, maxilla articulations (frontomaxillary, nasomaxillary, zygomaticomaxillary sutures), and zygomaticotemporal regions. Lines[20] attributed the pressure to frontomaxillary, zygomaticotemporal, zygomaticofrontal, and zygomaticomaxillary sutures; Timms[1] suspected the midpalatal suture and Revelo and Fishman[21] suspected zygomatic area and maxillary articulations, while Shetty et al.[22] and Lanigan and Mintz[23] named the midpalatal and pterygomaxillary sutures as the major buttresses.

During our study, other sutures implicated as important contributors to RME could not be visualized as precisely as the midpalatal sutures as a result of complex regional anatomy or because the suture was too thin to trace. Therefore, we measured the bone density at several locations important in RME. The region designated as the posterior maxillary buttress includes the pterygomaxillary region. The medial max-

illary buttress includes the zygomatic processes, and the anterior maxillary buttress includes the nasal area.

We were unable to find correlations between density and skeletal measurements or between density and AW or CW. Among the dental measurements, ImA was statistically highly significantly correlated ($P < .01$). A change in ImA may reflect alveolar bending, while tooth movement is negligible because of hyalinization within alveolar bone. Our results show a 32.1–43.3% correlation between density measurements and ImA increase. According to the calculated equation models, the ImA increase corresponding to specific skeletal density can be estimated. However, the variables were not distributed linearly, which may reflect the CT slice thickness and other factors (such as suture properties, appliance type, generated forces, and interaction between the forces and skeletal and soft tissues) that affect skeletal and dental RME outcomes. Furthermore, the number of subjects is an important limitation of this study affecting the data distribution used to formulate the model equation. Unfortunately, CT is not a routine diagnostic tool and has considerable adverse effects. The data used in this study comprised archived material obtained approximately 10 years ago when CBCT was uncommon; since then, new CT procedures have not been performed.

Bone and suture mineral densities may provide clues about the growth and resistance of skeletal components, but they are inadequate for providing measurable diagnostic information characterizing the maxillofacial area and for guiding the decision to elect SARME.

CONCLUSIONS

- CT is a reliable method with which to measure mineral density. Bone and suture density is one component of maxillary resistance to RME and affects the ImA increase.
- There is a highly significant correlation between the suture and skeletal density (HU) and the ImA increase.
- However, density measurements are not the sole or definitive indicator predicting RME outcome.

REFERENCES

1. Timms DJ. *Rapid Maxillary Expansion*. Chicago, Ill.: Quintessence Publishing; 1981:91–94.
2. Acheson RM. A method of assessing skeletal maturity from radiographs; a report from the Oxford child health survey. *J Anat*. 1954;88:498–508.
3. Litsas G, Ari-Demirkaya A. Growth indicators in orthodontic patients. Part 2: comparison of cervical bone age to hand-wrist skeletal age. Relationship with chronological age. *Eur J Paediatr Dent*. 2010;11:176–180.
4. Wehrbein H, Yildizhan F. The mid-palatal suture in young adults. A radiological-histological investigation. *Eur J Orthod*. 2001;23:105–114.
5. Walker L, Enciso R, Mah J. Three-dimensional localization of maxillary canines with cone-beam computed tomography. *Am J Orthod Dentofacial Orthop*. 2005;128:418–423.
6. Hamada Y, Kondoh T, Noguchi K. Application of limited cone beam computed tomography to clinical assessment of alveolar bone grafting: a preliminary report. *Cleft Palate Craniofac J*. 2005;42:128–137.
7. Poggio PM, Incorvati C, Velo S, Carano A. ''Safe zones'': a guide for miniscrew positioning in the maxillary and mandibular arch. *Angle Orthod*. 2006;76:191–197.
8. Garrett BJ, Caruso JM, Rungcharassaeng K, Farrage JR, Kim JS, Taylor GD. Skeletal effects to the maxilla after rapid maxillary expansion assessed with cone-beam computed tomography. *Am J Orthod Dentofacial Orthop*. 2008;134:8.e1–8.e11.
9. Schlegel KA, Kinner F, Schlegel KD. The anatomic basis for palatal implants in orthodontics. *Int J Adult Orthod Orthognath Surg*. 2002;17:133–139.
10. Persson M, Thilander B. Palatal suture closure in man from 15 to 35 years of age. *Am J Orthod*. 1977;72:42–52.
11. Korbmacher H, Schilling A, Püschel K, Amling M, Kahl-Nieke B. Age-dependent three-dimensional microcomputed tomography analysis of the human midpalatal suture. *J Orofacial Orthop*. 2007;68:364–376.
12. Schwarz MS, Rothman SL, Rhodes ML, Chafetz N. Computed tomography: part I. Preoperative assessment of the mandible for endosseous implant surgery. *Int J Oral Maxillofac Implants*. 1987;2:5.
13. Hilgers ML, Scarfe WC, Scheetz JP, Farman AG. Accuracy of linear temporomandibular joint measurements with cone beam computed tomography and digital cephalometric radiography. *Am J Orthod Dentofacial Orthop*. 2005;128:803–811.
14. Lagravère MO, Carey J, Toogood RW, Major PW. Three-dimensional accuracy of measurements made with software on cone-beam computed tomography images. *Am J Orthod Dentofacial Orthop*. 2008;134:112–116.
15. Misch KA, Yi ES, Sarment DP. Accuracy of cone beam computed tomography for periodontal defect measurements. *J Periodontol*. 2006;77:1261–1266.
16. Norton MR, Gamble C. Bone classification: an objective scale of bone density using the computerized tomography scan. *Clin Oral Implants Res*. 2001;12:79–84.
17. Shahlaie M, Gantes B, Schulz E, Riggs M, Crigger M. Bone density assessments of dental implant sites: 1. Quantitative computed tomography. *Int J Oral Maxillofac Implants*. 2003;18:224–231.
18. Marquezan M, Lau TC, Mattos CT, et al. Bone mineral density. *Angle Orthod*. 2012;82:62–66.
19. Haas AJ. Rapid expansion of the maxillary dental arch and nasal cavity by opening the midpalatal suture. *Angle Orthod*. 1961;31:73–90.
20. Lines PA. Adult rapid maxillary expansion with corticotomy. *Am J Orthod*. 1975;67:44–56.
21. Revelo B, Fishman SL. Maturational evaluation of ossification of the midpalatal suture. *Am J Orthod*. 1994;3:288–292.
22. Shetty V, Caridad JM, Caputo AA, Chaconas SJ. Biomechanical rationale for surgical-orthodontic expansion of the adult maxilla. *J Oral Maxillofac Surg*. 1994;52:742–749.
23. Lanigan D, Mintz S. Complication of surgically assisted rapid palatal expansion: review of the literature and report of a case. *J Oral Maxillofac Surg*. 2002;60:104–110.